

Measurement of the Energy Spectrum of Cosmic Rays above 3×10^{17} eV at the Pierre Auger Observatory

Ioana C. Mariş*

Institute Lagrange de Paris, LPNHE, Paris, France[†]

E-mail: ioanamaris@ugr.es

The Pierre Auger Collaboration

Observatorio Pierre Auger, Av. San Martín Norte 304, 5613 Malargüe, Argentina

full author list: www.auger.org/archive/authors_2013_06.html

We report the measurement of the flux of cosmic rays with unprecedented precision and statistics using data collected at the Pierre Auger Observatory until 31 December 2012. The fluorescence observation of the air-showers provides intrinsically a calorimetric energy measurement. Based on the hybrid nature of the experiment, the energy scale for the surface detector is obtained with minimal use of Monte Carlo simulations. The energy spectrum deduced with the more denser array of 750 m, which provides the extension of the energy range from 1.5×10^{18} eV down to 3×10^{17} eV will be emphasised. The spectral features are presented in detail and the systematic uncertainties are addressed.

The European Physical Society Conference on High Energy Physics -EPS-HEP2013

18-24 July 2013

Stockholm, Sweden

*Speaker.

[†]now: University of Granada, Spain

1. Introduction

To develop a complete theory on the origin of cosmic rays the energy spectrum from above 10^{14} eV up to the highest energies should be explained. At around 10^{15} eV a steepening of the energy spectrum, *the knee*, has been long established [1]. The KASCADE(-Grande) results have shown that this feature is caused by a steepening of the energy spectra of light elements [2], and recently the presence of a second change in the energy spectrum of light elements, at about 10^{17} eV [3] has been observed. In the energy region between 10^{17} eV and 3×10^{18} eV (where a flattening of the energy spectrum starts, *the ankle*) the transition between the galactic to extra-galactic origin of cosmic rays is expected. At the highest energies, above 5×10^{19} eV the flux is highly suppressed, due to propagation of the cosmic rays through the medium and/or caused by the maximum acceleration energy at their origin.

The measurement of the energy spectrum performed at the Pierre Auger Observatory extends from 3×10^{17} eV up to the highest energies. The recent usage of the data recorded with a denser sub-array has allowed the extension of the energy spectrum at lower energies in the region where the current smaller experiments, like KASCADE-Grande, run out of statistics. Also taking the advantage of the hybrid measurement performed at the Pierre Auger Observatory, the input from Monte-Carlo simulations is minimal. The energy spectrum will be complemented by the extension of the measurement of the maximum of the air-shower development to lower energies with the enhancement of the fluorescence telescopes, the High Elevation Auger Telescope (HEAT). We describe the measurement of the flux of the cosmic rays above 3×10^{17} eV, with an emphasis on the energy determination. The measurement of the energy using data recorded by the fluorescence detector has greatly improved in the last year, the systematic uncertainty decreased from 22% to 14%.

2. Reconstruction of the energy of cosmic rays

The Pierre Auger Observatory is designed as an hybrid detector: a surface detector (SD) with more than 1660 water-Cherenkov stations placed on a triangular grid covering 3000 km^2 and a fluorescence detector (FD) made of 27 optical telescopes grouped in five buildings, observing the atmosphere above the array. The detailed description of the Observatory can be found in [4, 5, 6]. The surface detector array is composed of water Cherenkov detectors with a separation of 1500 m. A sub-sample of the array includes 71 detectors placed at a distance of 750 m to each other. The measurement of the signal produced by the particles that reach the ground cannot provide a direct measurement of the energy of the primary cosmic rays. Therefore the energy is calculated by cross-calibrating an energy estimator with the fluorescence detector determination, by employing air-showers that were measured in coincidence with the two detectors (called golden hybrid events).

The charged particles from the air-showers excite the nitrogen molecules which then through the de-excitation produce fluorescence light. The emission is isotropic and the photons after propagating through the atmosphere are observed with the telescopes. The energy of the primary cosmic ray is then calculated by integrating the energy deposit in the atmosphere. The systematic uncertainty of the energy contains contributions starting from the physical process of producing the photons, the atmosphere propagation, the calibration and the light collection at the telescopes to the

	σ_E/E (2011)	σ_E/E (2013)	$\Delta E/E$ (at 1 EeV)
Fluorescence yield	14%	3.6%	-8.2%
FD calibration	9.5%	9.9%	7.8%
Atmosphere	5.1%-7.6%	3.4%-6.2%	-
FD profile reconstruction	10%	6.5%-5.6%	11.6%
Invisible energy	4%	3%-1.5%	4.6%
Total (including not listed contributions)	22%	14%	15.6%

Table 1: Systematic uncertainties on the energy scale and the changes on the energy at 1 EeV [9, 10].

reconstruction algorithms. There has been a big progress in the last year regarding the systematic uncertainty, reducing it from 22% to only 14%. The largest contribution, from the fluorescence yield absolute normalization reduced from 14% [7] to 4% by using the high precision measurements from [8]. A better understanding of the light correction at the telescopes and the development of a maximum likelihood fit taking into account the fluctuations of the signal in each PMT has improved the uncertainty coming from the reconstruction from 10% to less than 6.5%. A list of the systematic uncertainties on the energy is given in Table 2. These changes have induced also an energy-dependent shift of 15% at 1 EeV and 10% at 10 EeV. The energy resolution is between 7% and 8% with the main contributions from the aerosol optical depth and the statistical uncertainty from the longitudinal profile fit. The hybrid data, i.e. the events measured by the fluorescence detector for which the information from one surface detector is used to constrain the geometry reconstruction, are used to determine the energy spectrum above 1 EeV.

The surface detectors have access just to the particles that reach the ground. From the time of arrival of the particles the air-shower direction is reconstructed. Depending on the amount of matter traversed in the atmosphere the electromagnetic component of the air-showers is attenuated, for very inclined air-showers being negligible with respect to the muonic component. Therefore the data set from the surface detector is divided on two sets: air-showers with zenith angles smaller than 60 degrees and inclined events with the arrival direction between 62 and 80 degrees. For the vertical events we derive the energy estimator as the value of the lateral distribution function at a fixed distance from the axis. In order to minimize the assumptions of the lateral distributions an optimal distance can be defined depending on the spacing between detectors. In case of the 750 m array the energy estimator is obtained at 450 m, $S(450)$, while for the 1500 m array it is $S(1000)$, at 1000 m. The dependency on the zenith angle of these estimators, caused by the attenuation in the atmosphere is corrected using the hypothesis of a constant flux of cosmic rays as a function of the local coordinates, leading to two new variables S_{35} and S_{38} respectively. The reconstruction of the inclined events is based on a detailed modeling of the two dimensional muon density on the ground. The energy estimator, N19, is obtained by taking as a reference the normalization of the footprint of proton initiated air-showers with an energy of 10^{19} eV and it is independent of the zenith angle.

To convert S_{35} , S_{38} and N19 to energy we use golden hybrid events: a sub-sample of the hybrid events which are independently triggered and reconstructed with the SD. We are selecting high quality longitudinal profiles, observed during a time period with clear atmosphere, with a cloud coverage of less than 25%. Deeply penetrating air-showers would produce a larger signal on

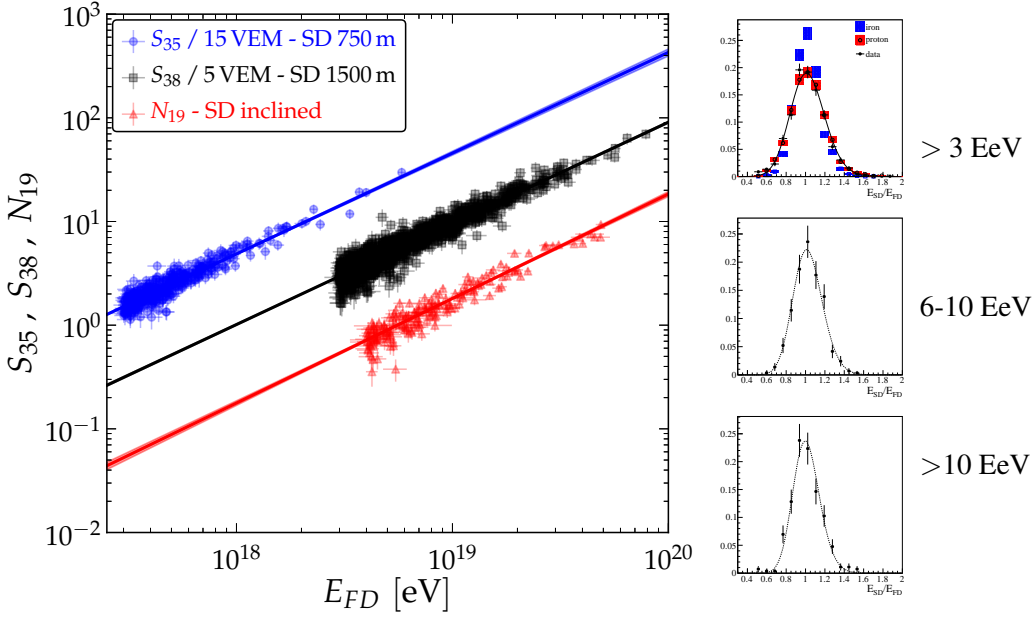


Figure 1: (left) The correlation between the energy estimators as deduced from the surface array and the energy obtained with the fluorescence detectors. [11, 12] (right) The ratio between the energies reconstructed with the hybrid and the surface detector data (1500 m) for different energy intervals. In the top plot the distribution is compared with MC for the events with an energy larger than 3 EeV (see text).

SD data set	1500 m vertical	1500 m inclined	750 m vertical
Zenith angle [°]	0 – 60	62 – 80	0 – 55
Energy calibration (A) [EeV]	0.190 ± 0.005	5.61 ± 0.1	$(1.21 \pm 0.07) \cdot 10^{-2}$
Energy calibration (B)	1.025 ± 0.007	0.985 ± 0.02	1.03 ± 0.02
Threshold energy E_{eff} [eV]	3×10^{18}	4×10^{18}	3×10^{17}
Data taking period	01/2004 - 12/2012	01/2004 - 12/2012	08/2008 - 12/2012
Exposure [km ² sr yr]	31645 ± 950	8027 ± 240	79 ± 4

Table 2: The experimental parameters describing data of the surface detector measurements at the Pierre Auger Observatory. For the explanation of the energy calibration parameters and the hybrid data set see text.

the ground than shallow ones. Thus, in order to reduce a possible mass composition bias we apply strict cuts on the fiducial field of view which assure an equal hybrid trigger probability for different primaries. The correlation functions, $E_{\text{SD750}; \text{SD1500}; \text{SDinclined}} = A \cdot (S_{35}; S_{38}; N_{19})^B$ are obtained by maximizing the likelihoods and are in all the three cases almost linear (see Table 2 and Fig. 1 (left)). In the case of the 750 m array the usage of HEAT data has increased the statistics by a factor 3 and thus reducing the energy systematic uncertainty due to the energy calibration. For the case of the 1000 m array due to the high number of events, this systematic uncertainty is below 2%. The energy resolution for the surface detectors is dependent on energy, evolving from 16% at 3 EeV to 12% at the highest energies. Knowing that the FD energy resolution is 7-8% the SD energy resolution can be obtained from data only. In order to account for bin to bin migrations in the energy spectrum due to the trigger effects and this finite resolution a forward folding procedure is used. To generate

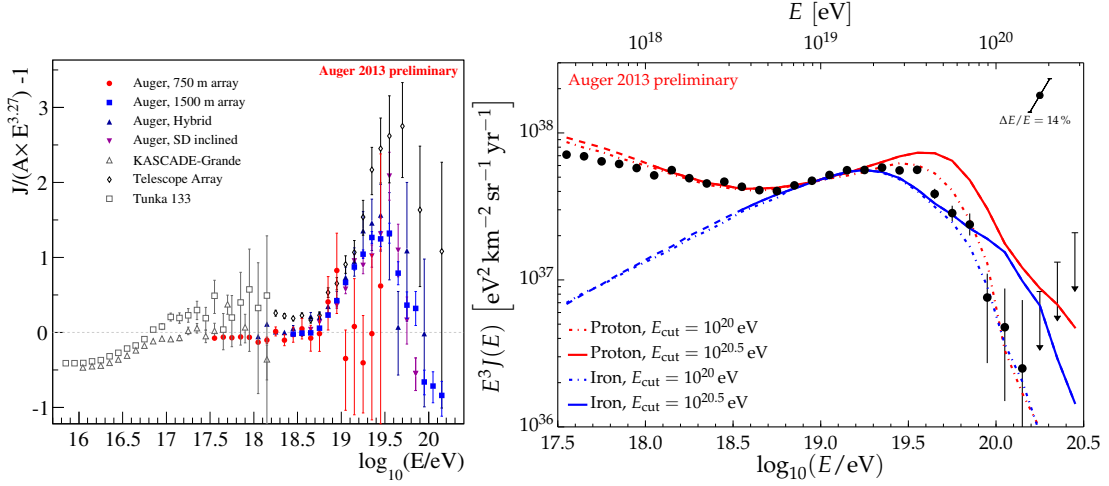


Figure 2: (left) Energy spectra of the 750 m and 1500 m surface arrays, and the hybrid one as obtained at the Pierre Auger Observatory. The KASCADE Grande [14], the Telescope Array [15] and Tunka [16] measurements are also illustrated. (right) The energy spectrum compared to energy spectra predicted by different astrophysical scenarios [13].

the energy migration matrices we use Monte Carlo simulations generated with CORSIKA (QGSJet II.03 and Fluka) and Geant4 detector simulations assuming a mixed composition (50% proton and 50% iron). The very good agreement between data and Monte Carlo is illustrated in Fig. 1 (right) for energies larger than 3 EeV.

3. Energy spectrum

The energy spectrum measurements obtained with data up to end of 2012 are illustrated in Fig. 2(left). The vertical SD measurement dominates in terms of statistics, with an integrated exposure of $31645 \pm 950 km^2 sr yr$. Due to the smaller solid angle the measurement using the inclined SD events has an integrated exposure four times smaller. The integrated exposures and the energy threshold for full trigger efficiency for the SD measurements are given in Table 2. The hybrid measurement of the energy spectrum starts at an energy of 1 EeV overlapping in the lower energy region with the one obtained with the 750 m array and above 3 EeV with the 1500 m array measurement. Over almost the entire energy range there are two independent measurements from the Pierre Auger Observatory data. In the same Figure the energy spectra measured at the KASCADE-Grande, Tunka and Telescope Array experiments are illustrated. Given the energy systematic uncertainties the measurements from different experiments are in a good agreement.

The energy spectra are combined using a method that takes into account the systematic uncertainties of the individual measurements. The resulting combined spectrum is shown in Fig. 2(right). The spectrum exhibits a flattening at $\log_{10}(E_a/eV) = 18.7 \pm 0.01 \pm 0.02$ from a spectral index of $3.23 \pm 0.01 \pm 0.07$ to $2.63 \pm 0.02 \pm 0.04$ and at the highest energies a flux suppression with a significance of more than 20σ . The energy spectrum is compared to shapes of fluxes predicted by extra-galactic astrophysical scenarios in the same figure, assuming pure proton or iron composition. The flux at Earth depends on the spectrum of particles produced at the source, in these ex-

amples assumed -2.35 for proton and -2.3 for iron, on the cosmological evolution of sources, $m=5$ (proton) and $m=0$ (iron) and on the propagation. The theoretical lines have been produced using CRPropa [17] and validated with SimProp [18]. The maximum energy of the source was set to 100 EeV and 300 EeV, the former describing better the data in the flux suppression region. The energy spectrum alone cannot distinguish between different hypothesis, but it has to be complemented with a mass composition measurement [19].

4. Conclusions

The energy spectrum above 0.3 EeV has been measured at the Pierre Auger Observatory with a very large number of events and thus the spectral features are determined with an unprecedented precision. The progress in understanding the fluorescence detector and reconstruction and the new measurements of the fluorescence yield have allowed us to achieve a reduction of the energy systematic uncertainty from 22% to 14%. The spectrum alone cannot shed light on the origin of cosmic rays, and thus a measurement of the evolution of the mass composition of the UHECRs in the whole energy range is required. The data from the fluorescence detectors can provide this up to the flux suppression energy region, while a possible upgrade of the surface detector might help in elucidating the composition at the highest energies.

References

- [1] G.V. Kulikov and G.B. Khristiansen, Soviet Physics JETP 35 3 (1959)
- [2] T. Antoni et al. Astropart. Phys., 24, 1 (2005)
- [3] A. Haungs, these proceedings
- [4] The Pierre Auger Collaboration, Nucl. Instrum. Meth. **A523** (2004) 50.
- [5] I. Allekotte et al., Nucl. Instrum. Meth. **A586** (2008) 409.
- [6] The Pierre Auger Collaboration, Nucl. Instrum. Meth. **A620** (2010) 227.
- [7] M. Nagano et al. Astropart.Phys. **28**(2007) 41.
- [8] M. Ave et al., Astropart. Phys **42**(2013) 90.
- [9] The Pierre Auger Collaboration, R. Pesce, Proc. 32nd ICRC,China, **2** (2011) 214, arXiv:1107.4809.
- [10] The Pierre Auger Collaboration, V. Verzi, Proc. 33rd ICRC, Brazil(2013), arXiv:1307.5059
- [11] The Pierre Auger Collaboration, A. Schultz, Proc. 33rd ICRC, Brazil(2013), arXiv:1307.5059
- [12] The Pierre Auger Collaboration, D. Ravignani, Proc. 33rd ICRC, Brazil(2013), arXiv:1307.5059
- [13] The Pierre Auger Collaboration, A. Letessier-Selvon, Proc. 33rd ICRC, Brazil(2013)
- [14] The KASCADE-Grande Collaboration, Phys. Rev. Lett. **107** (2011) 171104.
- [15] T. Abu-Zayyad *et al.*, ApJ **768** (2013) L1.
- [16] The Tunka Collaboration, Proc. 32nd ICRC, 1 (2011) 209.
- [17] K.H. Kampert et al., Astropart. Phys. **42** (2013) 41.
- [18] R. Aloisio et al., JCAP **10** (2012) 007.
- [19] The Pierre Auger Collaboration, S. Andringa, these proceedings.